Nanoscale Res Lett (2007) 2:391–396
DOI 10.1007/s11671-007-9072-6

NANO EXPRESS

ZnO Nanorods via Spray Deposition of Solutions Containing Zinc Chloride and Thiocarbamide

Tatjana Dedova · Olga Volobujeva · Jelena Klauson · Arvo Mere · Malle Krunks

Received: 16 May 2007 / Accepted: 12 June 2007 / Published online: 19 July 2007

Abstract In this work we present the results on formation of ZnO nanorods prepared by spray of aqueous solutions containing $ZnCl_2$ and thiocarbamide (tu) at different molar ratios. It has been observed that addition of thiocarbamide into the spray solution has great impact on the size, shape and phase composition of the ZnO crystals. Obtained layers were characterized by scanning electron microscopy (SEM) equipped with energy selected backscattered electron detection system (ESB), X-ray diffraction (XRD) and photoluminescence spectroscopy (PL). Small addition of thiocarbamide into $ZnCl_2$ solution ($ZnCl_2$:tu = 1:0.25) supports development of significantly thinner ZnO nanorods with higher aspect ratio compared to those obtained from $ZnCl_2$ solution. Diameter of ZnO rods decreases from 270 to 100 nm and aspect ratio increases from ~2.5 to 12 spraying $ZnCl_2$ and $ZnCl_2$:tu solutions, respectively. According to XRD, well crystallized (002) orientated pure wurtzite ZnO crystals have been formed. However, tiny 'spot'—like formations of ZnS were detected on the side planes of hexagonal rods prepared from the thiocarbamide containing solutions. Being adsorbed on the side facets of the crystals ZnS inhibits width growth and promotes longitudinal *c*-axis growth.

Keywords ZnO nanorods · Spray pyrolysis · Thiocarbamide · Zinc chloride · Growth mechanism · SEM · PL

T. Dedova (✉) · O. Volobujeva · J. Klauson · A. Mere · M. Krunks
Department of Materials Science, Tallinn University of Technology, Ehitajate tee 5, Tallinn 19086, Estonia
e-mail: dedova@staff.ttu.ee

Introduction

One-dimensional zinc oxide (ZnO) nanostructures have been the subject of intense research in the past few years due to their unique properties and thus potential wide-ranging applications in a variety of fields such as solar cells [1–3], sensors [4, 5], short-wavelength light emitting and field effect devices [6, 7], Schottky diodes [8, 9], and coating materials [10, 11]. Controlling the size and shape of nanocrystalline materials is a crucial issue in nanoscience research. The ordered growth and high surface area of one-dimensional ZnO nanorods are desirable as it would provide significant enhancement of the devices efficient functioning.

Several techniques have been developed for the fabrication of the 1D nanostructures, including metal organic chemical vapor [12, 13], pulsed laser [14, 15], electrochemical deposition techniques [16, 17], vapor–liquid–solid [18, 19] and wet chemical methods [20–22].

Chemical spray pyrolysis has the advantage over the other methods being a less time and expenses consumable, catalyst and template free method to prepare ZnO nanostructures.

In our previous works [23–25] we have demonstrated the possibility to synthesize high quality *c*-axis orientated ZnO rods by a simple spray pyrolysis deposition method using zinc chloride aqueous solutions as a single precursor. It was found that size, shape and aspect ratio of ZnO nanostructures prepared by spray pyrolysis strongly depend on the $ZnCl_2$ concentration, deposition time, growth temperature and the substrate properties. In solution systems of wet-growth methods, the morphology of grown ZnO crystals has been controlled by the reaction conditions and the presence of various additives. In order to obtain the desired crystals size, shape and aspect ratios of final ZnO

product by solution-based methods, so-called surfactant or capping molecules are added to the solution. They can manipulate the growth kinetics and determine the final morphologies being adsorbed to the certain crystal planes. For instance, hexamine [26] and oleic acid [27] inhibit [0110] and promotes the [0001] growth resulting in thinner and high-aspect ratio rods. Additives such as sodium dodecyl sulfate (SDS) [28], triethanolamine (TEA) [28], citric acid [29] retard the growth along the *c*-axis direction resulting in a disk-like structures or platy forms.

In this study, we demonstrate the influence of thiocarbamide addition to the zinc chloride solution on development of ZnO rods, their dimensions, phase composition, morphological, structural and photoluminescence (PL) properties. The formation chemistry and growth mechanism of the ZnO nanorods is proposed. To our best knowledge this is the first report on preparation of ZnO nanorods from thiourea and zinc chloride solution system.

Experimental

ZnO nanorods were deposited using pneumatic spray pyrolysis technique. Spray aqueous solution was prepared by mixing of $ZnCl_2$ and thiocarbamide (tu) at the molar ratios (Zn:tu) of 1:0 ($ZnCl_2$ solution without tu), 1:0.05, 1:0.1, 1:0.25 and 1:0.5. The $ZnCl_2$ concentration in solutions was adjusted to 0.1 and 0.05 mol/L. The resultant solution in amount of 50 mL was pulverized onto the SnO_2 covered glass and soda-lime bare glass substrates mounted on a soldered tin bath.

The deposition temperature (T_S, temperature at substrate surface) was kept at 520 °C and controlled through the tin bath temperature using an electronic temperature controller. The solution flow rate and gas pressure were kept constant at 2.5 mL/min and 8 L/min, respectively; air was used as the carrier gas supplied by filter equipped oil-free compressor.

The structural characterization of deposited films structures was carried out on Bruker AXS D5005 diffractometer (monochromatic Cu Kα radiation, λ = 1.54056 Å) in 2θ range 20–60 deg with the step of 0.04 deg and counting time 2 s/step. The reflections were identified by JCPDS files.

The surface morphology and film cross-section micrographs were taken by a high-resolution scanning electron microscope ZEISS Ultra 55 equipped with an Energy Backscattered electron (ESB) detector to determine the elemental composition difference. For the room-temperature photoluminescence measurements, a He–Cd laser with a wavelength of 325 nm was used for excitation. The PL spectra were taken with a SPM-2 grating monocromator (f = 0.4 m) and the signal was detected with a photomultiplier tube. The measurements were made in the 310–620 nm range.

Results and Discussion

Effect of Thiocarbamide on Morphology of ZnO Nanorods

Figure 1 illustrates the SEM images of ZnO nanorods deposited onto SnO_2 covered glass substrates by the spray pyrolysis process using zinc chloride (Fig. 1a) and zinc chloride containing thiocarbamide additive adjusting the molar ratio of Zn:tu = 1:0.25 (Fig. 1b). Zinc chloride concentration in solution of 0.05 mol/L and deposition temperature of 520 °C were kept constant for both samples. As can be seen, thiocarbamide additive drastically influences the ZnO nanorods dimensions. The diameters of rods decreased from 300 to 120 nm, and length increased from 500 to 700 nm, resulting in increase of the aspect ratio more than three times for the samples deposited from thiourea containing solution.

In our previous work [25] we have observed that in order to grow well-aligned ZnO nanorods on SnO_2, it is essential to use the precursor concentration in solutions below than 0.1 mol/L. Since the deposition of 0.1 mol/L solutions resulted in fat ZnO crystals with low aspect ratio.

Strikingly, elongated high aspect ratio (~12) ZnO nanorods has been observed using thiourea (Zn:tu = 1:0.25, molar ratios) in the $ZnCl_2$ solution with concentration of 0.1 mol/L (See Fig. 2).

The comparison of average diameters, lengths and aspect ratios of the sprayed ZnO nanocrystals depending on

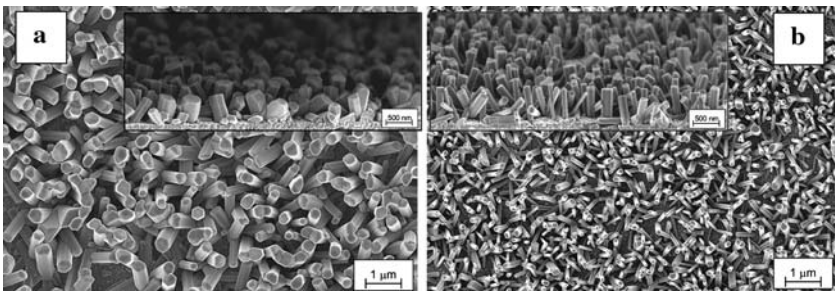

Fig. 1 SEM micrographs from the surface and cross-sectional views (in inset) of ZnO samples deposited using $ZnCl_2$ solutions: (**a**) without and (**b**) containing thiourea at Zn:tu molar ratio of 1:0.25; $[Zn^{2+}]$ = 0.05 mol/L

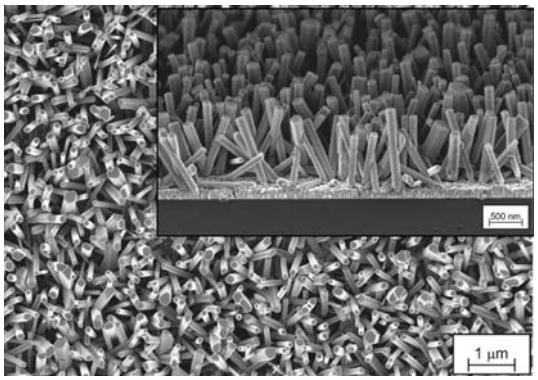

Fig. 2 The SEM surface and cross-sectional views (inset) images of ZnO nanorods obtained from solution with thiourea addition at molar ratio of Zn:tu = 1:0.25, $[Zn^{2+}]$ = 0.1 mol/L

the $ZnCl_2$ concentration and content of thiourea additive are summarized in Table 1.

As it could be seen from Table 1, thiocarbamide addition generally leads to the formation of thinner rods with higher aspect ratio compared to those deposited from $ZnCl_2$ solution. However, amount of thiocarbamide in solution is extremely important factor which determines the final rods dimensions. For instance, too low (Zn:tu = 1:0.05) or too high (Zn:tu = 1:0.5) amount of added thiourea results in thicker and low aspect ratio rods. The molar ratio of Zn:tu = 1:0.25 seems to be optimal in order to grow highest aspect ratio nanorods.

Structural Properties and Phase Composition of ZnO Layers

Figure 3 shows the XRD pattern of the sprayed nanorods prepared from solution containing thiocarbamide with Zn:tu ratio = 1:0.25 and $[Zn^{2+}]$ = 0.1 mol/L. Strong and sharp diffraction peak at $2\theta = 34.4°$ corresponds to the (002) reflection of ZnO wurtzite phase (JCPDS 36-1451) indicating preferred orientation in the *c*-axis direction. No other peaks related to any impurity phases were observed in this XRD graph.

Table 1 The average diameters, lengths and aspect ratios of the sprayed ZnO nanorods deposited from solutions without and with thiourea at two different concentrations of $ZnCl_2$—0.05 mol/L and 0.1 mol/L

$[Zn^{2+}]$	Zn:tu	Length (L)	Diameter (D)	Aspect ratio (L/D)
C = 0.05	1:0	500	300	1.7
	1:0.25	700	120	6
C = 0.1	1:0	700	270	2.5
	1:0.05	750	250	3
	1:0.1	800	200	4
	1:0.25	1,200	100	12
	1:0.5	700	250	3

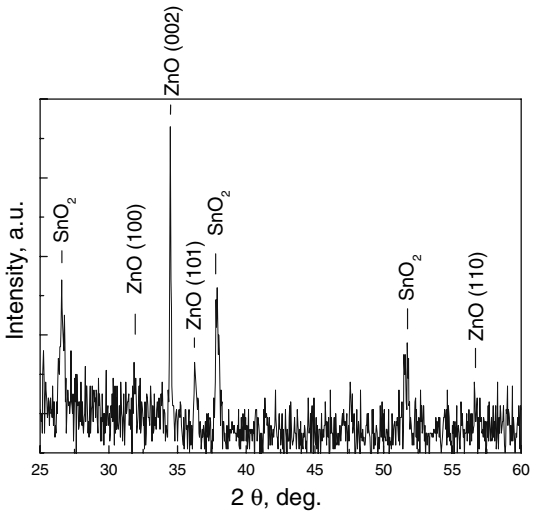

Fig. 3 XRD pattern of the samples deposited from solutions containing $ZnCl_2$ and thiocarbamide (Zn:tu = 1:0.25), $[Zn^{2+}]$ = 0.1 mol/L

However some "spots" like contaminations on the planes of well-formed hexagonal crystals could be observed in high magnification SEM micrograph (Fig. 4b). The colour contrast difference on ESB analysis (Fig. 4a) clearly indicates that the elemental composition of 'spots' differ from the ZnO rods. As the formation of spots on ZnO lateral facets has been found only in the case of thiourea containing spray solutions, obviously the origin of spots is issued from the thiourea. Here should be pointed out that the upper planes of the crystals are clean from the contaminants having very smooth well-developed hexagon.

From earlier reports [30–32] it is known that $ZnCl_2$ and thiourea are main precursors for ZnS thin films deposition by spray pyrolysis. To control whether the "spots" belong

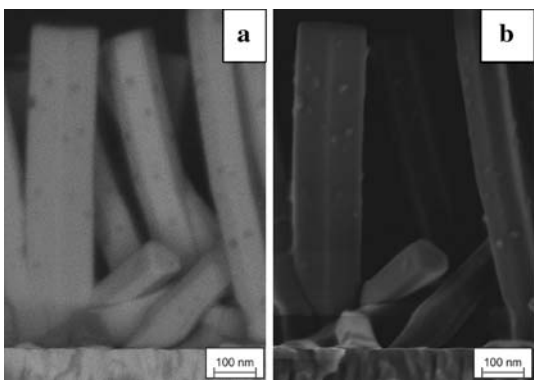

Fig. 4 (**a**) ESB and (**b**) high magnification SEM cross-sectional micrographs of the sample deposited from solutions containing $ZnCl_2$ and thiocarbamide (Zn:tu = 1:0.25), $[Zn^{2+}]$ = 0.1 mol/L

to ZnS phase we prepared the ZnO samples increasing the content of tu in solution (molar ratio of Zn:tu = 1:0.5). According to SEM (not presented here) amount of spots on the crystal side planes has increased and well developed but thicker ZnO rods have been formed (see Table 1). Figure 5 presents the XRD pattern of this sample recorded using parallel beams.

Weak reflection at 2θ of 28.5°, detected in the XRD pattern, could be attributed to the (111) reflection of ZnS sphalerite phase. As it has been reported [33, 34], the $ZnCl_2$ and thiourea in an aqueous solution yield the complex compound—dichlorobis(thiourea)zinc with molecular formula $Zn(tu)_2Cl_2$, which decomposes with formation of zinc sulfide at temperatures above 300 °C [33, 34].

Development of ZnO Nanorods in Initial Stages of Growth: Growth Mechanism

To understand the growth mechanism of ZnO nanorods obtained with and without thiocarbamide addition into solution, their morphologies in the initial growth stages were recorded by SEM.

After 1 min reaction time, ZnO crystals with diameter of ~50 nm from $ZnCl_2$ solution (Fig. 6a) and ~70 nm from thiourea containing solution have been formed. The length and coverage of rods deposited using thiocarbamide additive is almost two times higher revealing the higher growth rate. Figure 6c and d shows the SEM images of the samples obtained when the reaction proceeded 5 min. Figure 6c clearly reveals that the diameters of the rods grown from $ZnCl_2$ has drastically increased (~150 nm) whereas length is only 200 nm. It also should be pointed out that two different types of ZnO crystals could be observed in this picture. Some of them are flat hexagonal prisms; others have pyramidal-like forms. It is known from the literature

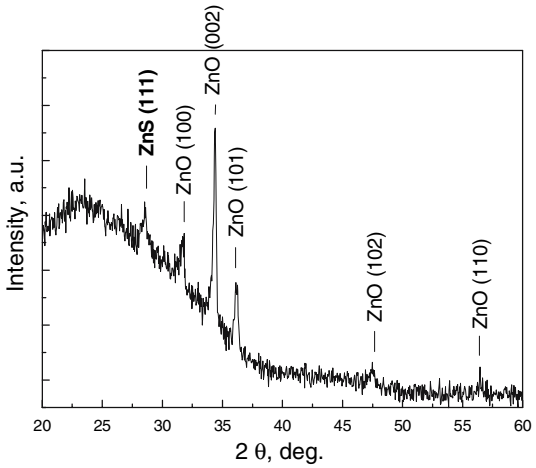

Fig. 5 XRD pattern of the sample obtained from solution containing $ZnCl_2$ and thiocarbamide (Zn:tu = 1:0.5), $[Zn^{2+}]$ = 0.1 mol. Diffractogram was recorded using parallel beams

that pyramidal planes are characteristic for moderate crystal growth being much lower than 002 direction growth [35]. At the final stage of the growth after 15 min, the coverage density has increased (Fig. 6e, f) for both types of solutions. Fat hexagonal prisms with pyramid crystals and elongated nanorods were obtained from the solutions containing $ZnCl_2$ (Fig. 6e) and $ZnCl_2$ with addition of thiocarbamide (Fig. 6f), respectively.

On the basis of the SEM and XRD results described above we propose the following mechanism (illustrated in Fig. 7) for the formation of ZnO nanorods in the presence of thiourea in the spray solutions.

It is known that in some crystallization processes the growth rate of a crystal facet can be inhibited by the addition of an impurity strongly adsorbing onto the growth front and thereby 'poisons' the incorporation of new molecules into that facet [36].

The ZnS particles, issued from the zinc–thiocarbamide complex decomposition being adsorbed onto the freshly formed ZnO side facets retard the crystal growth to the width thus promoting the longitudinal, *c*-axis growth (see Fig. 7).

Similar growth mechanism preventing the "width" growth and facilitating the *c*-axis growth has been observed for ZnO nanorod formation in chemical bath deposition using hexamine and oleic acid additives [26, 27].

In order to control whether the carbamide ($CO(NH_2)_2$), which molecular structure is very similar to thiocarbamide ($CS(NH_2)_2$), influences the ZnO crystals formation, we prepared some samples using urea instead of thiourea at the molar ratio of Zn to urea = 1:0.25. As a result, fat crystals have been formed. This is the next argument that the ZnS pieces originated from thiourea addition affect the development of ZnO crystals.

PL Measurements

Room-temperature PL spectra of the samples prepared from the solutions without and with thiourea addition at molar ratio of Zn:tu = 1:0.25 are presented in Fig. 8.

ZnO rods deposited from $ZnCl_2$ solution exhibits dominating strong and sharp and near band edge (NBE) emission band centred at 3.25 eV (382 nm). According to the literature data, NBE or UV-emission typically results from the recombination of free or bound exciton [37, 38] indicating the high crystal quality of the material. The green emission band is absent in the spectrum of this sample. PL spectrum of the samples prepared from the solutions containing thiocarbamide shows decreased intensity of the UV-emission band and appearance of green-emission band at app. 2.4 eV (517 nm). The green emission band originates from the recombination of photo-generated hole with a singly ionized defect, such as oxygen vacancy [39, 40].

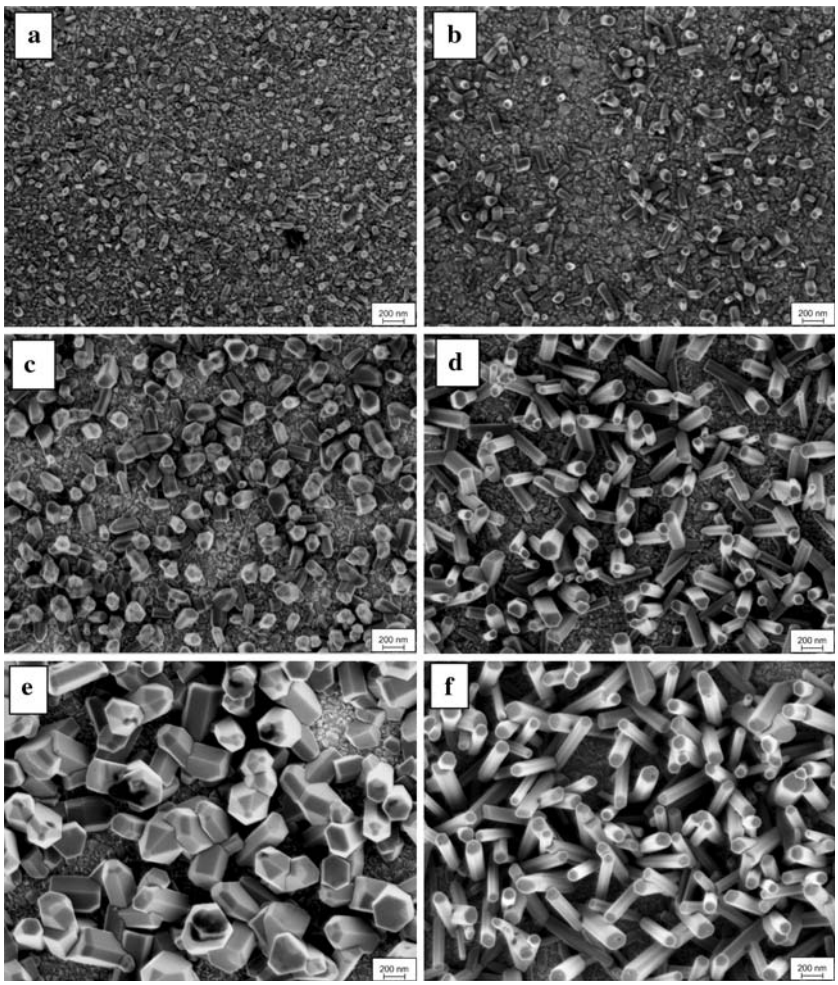

Fig. 6 SEM plain views of the samples deposited from $ZnCl_2$ solution are presented in the left column (**a**, **c**, **e**); and from tu containing solution at $ZnCl_2$:tu = 1:0.25 in the right column (**b**, **d**, **f**) using deposition times of 1 min (**a** and **b**); 5 min (**c** and **d**); 15 min (**e** and **f**). $[Zn^{2+}]$ = 0.1 mol/L was used in all experiments

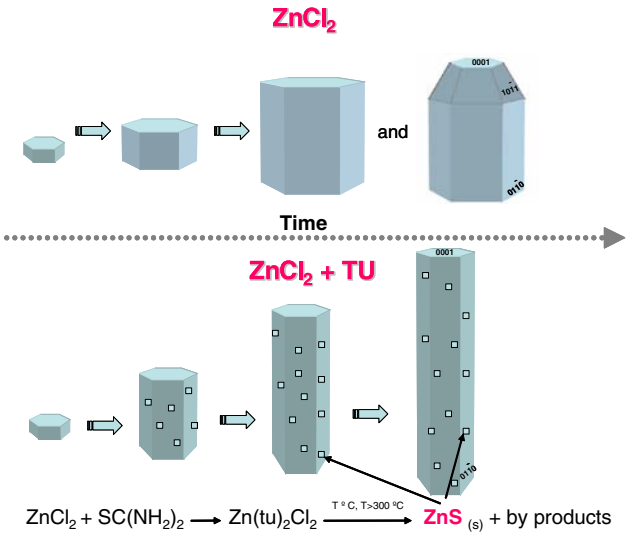

Fig. 7 Schematic illustration of the possible growth mechanism for the formation of ZnO nanorods from the $ZnCl_2$ solutions without and with thiourea

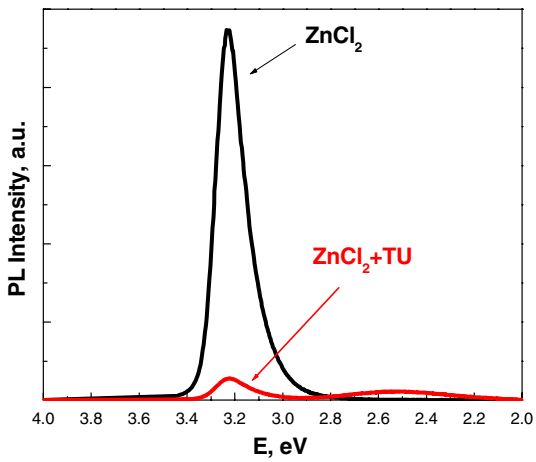

Fig. 8 Room-temperature PL spectra of the ZnO nanorods prepared from solutions of $ZnCl_2$ and $ZnCl_2$ containing thiocarbamide at molar ratio of Zn:tu = 1:0.25, $[Zn^{2+}]$ = 0.05 mol/L

According to some reports [4, 41–43] a higher intensity of the green emission observed from thinner nanorods is due to their higher surface-to-volume ratio. Taking into account that ZnO nanorods prepared with thiocarbamide additive contain some ZnS phase, the appearance of green-emission band and decreased intensity of the NBE band could be related to this impurity phase.

Conclusions

In conclusion, ZnO nanorods have successfully been synthesized via a simple and cost-effective spray pyrolysis route. Small addition of thiocarbamide into $ZnCl_2$ solution ($ZnCl_2$:tu = 1:0.25) supports development of significantly thinner ZnO nanorods with higher aspect ratio compared to those obtained from only $ZnCl_2$ solution. The diameter of ZnO rods decreases from 270 to 100 nm and aspect ratio increases from ~2.5 to 12 spraying $ZnCl_2$ and $ZnCl_2$:tu solutions, respectively. Structural analyses showed that the nanorods are *c*-axis orientated ZnO wurzite crystals. ZnS particles, issued from the zinc–thiocarbamide complex decomposition being adsorbed onto the freshly formed ZnO side facets, retard the crystal growth to the width thus promoting the longitudinal, *c*-axis growth. As a result, the intensity of NBE emission decreases and green-emission band appears in the room-temperature PL spectra of ZnO nanorod samples prepared by spraying of thiocarbamide containing solutions.

Acknowledgements This work is supported by the Estonian Ministry of Education and Science, Estonian Science Fundation Grant No. 6954 and Estonian Doctoral School of Materials Science and Technology. Authors would like to thank M. Grossberg for PL measurements.

References

1. P. Charoensirithavorn, S. Yoshikawa, Mater. Res. Soc. Symp. Proc. **974**, 0974-CC07-10 (2007)
2. K. Keis, L. Vayssieres, S.-E. Lindquist, A. Hagfeldt, Nanostruct. Mater. **12**, 487 (1999)
3. W.U. Huynh, J.J. Dittmer, A.P. Alivisatos, Science **29**, 2425 (2002)
4. (a) L. Liao, H.B. Lu, J.C. Li, H. He, D.F. Wang, D.J. Fu, C. Liu, (b) W.F. Zhang, J. Phys. Chem. C. **111**(5), 1900 (2007)
5. T. Shibata, K. Unno, E. Makino, Y. Ito, S. Shimada, Sens. Actuators A **102**, 106 (2002)
6. (a) W.I. Park, J.S. Kim, G.-C. Yi, (b) M.H. Bae, H.-J. Lee, App. Phys. Lett. **85**(21), 5052 (2004)
7. S.-H. Park, S.-H. Kim, S.-W. Han, Nanotechonology **18**, 055608 (2007)
8. (a) W.I. Park, G.-C. Yi, (b) J.-W. Kim, S.-M. Park, App. Phys. Lett. **82**(24), 4358 (2003)
9. (a) Y.W. Heo, L.C. Tien, D.P. Norton, S.J. Pearton, (b) B.S. Kang, F. Ren, J.R. LaRoche, App. Phys. Lett. **85**(15), 3107 (2004)
10. X.J. Feng, L. Jiang, Adv. Mater. **18**, 3063 (2006)
11. S. Yin, T. Sato, J. Mater. Chem. **15**, 4584 (2005)
12. W.I. Park, D.H. Kim, S.-W. Jung, G.-C. Yi, Appl. Phys. Lett. **80**, 4232 (2002)
13. J.Y. Park, D.J. Lee, Y.S. Yun, J.H. Moon, B.-T. Lee, S.S. Kim, J. Crystal Growth **276**, 158 (2005)
14. J.-H. Park, Y.-J. Choi, W.-J. Ko, I.-S Whang, J.-G. Park, Mater. Res. Soc. Symp. Proc. **848**, FF9.7.1 (2005)
15. (a) Z.W. Liua, C.K. Ong, (b) T. Yu, Z.X. Shen, Appl. Phys. Lett. **88**, 053110 (2006)
16. Y.C. Wang, M. Hon, Electrochem. Solid-State Lett. **5**, C53 (2002)
17. M.J. Zheng, Chem. Phys. Lett. **363**, 123 (2002)
18. M.H. Huang, Y. Wu, H. Feick, N. Tran, E. Weber, P. Yang, Adv. Mater. **13**, 113 (2001)
19. N. Pan, X. Wang, K. Zhang, H. Hu, B. Xu, F. Li, J.G. Hou, Nanotechnology **16**, 1069 (2005)
20. H. Zhu, D. Yang, H. Zhang, Inorg. Mater. **42**, 1210 (2006)
21. F. Li, Z. Li, F.J. Jin, Mater. Lett. **61**, 1876 (2007)
22. L. Vayssieres, Adv. Mater. **15**, 464 (2003)
23. M. Krunks, T. Dedova, I. Oja, Thin Solid Films **515**, 1157 (2006)
24. T. Dedova, M. Krunks, M. Grossberg, O. Volobujeva, I.O. Acik, Superlattices Microstruct. (2007) (in press, doi:10.1016/j.spmi.2007.04.010)
25. T. Dedova, M. Krunks, A. Mere, J. Klauson, O. Volobujeva, Mater. Res. Soc. Symp. Proc. **957**, 0957-K10-26 (2007)
26. (a) Z. Zhu, T. Andelman, M. Yin, (b) T.-L. Chen, (c) S.N. Ehrlich, (d) S.P. O'Brien, R.M. Osgood, J. Mater. Res. **20**(4), 1033 (2005)
27. A. Sugunan, H.C. Warad, M. Boman, J. Dutta, J. Sol–Gel Sci. Technol. **39**, 49 (2006)
28. P. Li, Y. Wei, H. Liu, X.-K. Wang, J. Solid State Chem. **178**, 855 (2005)
29. H. Zhang, D. Yang, D. Li, X. Ma, S. Li, D. Que, Cryst. Growth Design **5**, 547 (2005)
30. T. Dedova, M. Krunks, O. Volobujeva, I. Oja, Physica Status Solidic **2**(3), 1161 (2005)
31. B. Elidrissi, M. Addou, M. Regragui, A. Bougrine, A. Kachouane, J.C. Bernède, Mater Chem. Phys. **68**, 175 (2001)
32. H. H. Afifi, S.A. Mahmoud, A. Ashour, Thin Solid Films **263**, 248 (1995)
33. J. Madarász, P. Bombicz, M. Okuya, S. Kaneko, Solid State Ionics **439**, 141 (2001)
34. M. Krunks, J. Madarász, T. Leskelä, A. Mere, L. Niinistö, G. Pokol, J. Therm. Anal. Cal. **72**, 497 (2003)
35. D. Wang, C. Song, Z. Hu, W. Chen, X. Fu, Mater. Lett. **61**, 205 (2007)
36. T. Schilling, D. Frenkel, J. Phys.: Condens. Matter. **16**, S2029 (2004)
37. Y.C. Kong, D.P. Yu, B. Zhang, W. Fang, S.Q. Feng, Appl. Phys. Lett. **78**, 407 (2001)
38. M.H. Huang, Y. Wu, H. Feick, N. Tran, E. Weber, P. Yang, Adv. Mater. **13**, 113 (2001)
39. K. Vanheusden, W.L. Warren, C.H. Ceager, D.R. Tallant, J.A. Voigt, J. Appl. Phys. **79**, 7983 (1996)
40. M. Anpo, Y. Kubokawa, J. Phys. Chem. **88**, 5556 (1984)
41. J. Park, H.-H. Choi, R. K. Singh, Mat. Res. Soc. Symp. Proc. **776**, Q7.10.1 (2003)
42. F. Liu, P.J. Cao, H.R. Zhang, C.M. Shen, Z. Wang, J.Q. Li, H.J. Gao, J. Cryst. Growth **274**, 126 (2005)
43. G. Sun, M. Cao, Y. Wang, C. Hu, Y. Liu, L. Ren, Z. Pu, Mater. Lett. **60**, 2777 (2006)